VU VRIJE UNIVERSITEIT AMSTERDAM

VU Research Portal

Extramuscular myofascial force transmission alters substantially the acute effects of surgical aponeurotomy: assessment by finite element modeling

Yucesoy, Can; Koopman, Bart; Grootenboer, Henk; Huijing, Peter

published in
Biomechanics and Modeling in Mechanobiology
2007

document version
Publisher's PDF, also known as Version of record

Link to publication in VU Research Portal

citation for published version (APA)
Yucesoy, C., Koopman, B., Grootenboer, H., & Huijing, P. (2007). Extramuscular myofascial force transmission alters substantially the acute effects of surgical aponeurotomy: assessment by finite element modeling. *Biomechanics and Modeling in Mechanobiology*.

General rights
Copyright and moral rights for the publications made accessible in the public portal are retained by the authors and/or other copyright owners and it is a condition of accessing publications that users recognise and abide by the legal requirements associated with these rights.

- Users may download and print one copy of any publication from the public portal for the purpose of private study or research.
- You may not further distribute the material or use it for any profit-making activity or commercial gain
- You may freely distribute the URL identifying the publication in the public portal

Take down policy
If you believe that this document breaches copyright please contact us providing details, and we will remove access to the work immediately and investigate your claim.

E-mail address:
vuresearchportal.ub@vu.nl

Download date: 29. Mar. 2024

Biomechan Model Mechanobiol
DOI 10.1007/s10237-007-0084-z

ORIGINAL PAPER

Extramuscular myofascial force transmission alters substantially the acute effects of surgical aponeurotomy: assessment by finite element modeling

Can A. Yucesoy · Bart H. F. J. M. Koopman · Henk J. Grootenboer · Peter A. Huijing

Received: 3 July 2006 / Accepted: 4 April 2007
© Springer-Verlag 2007

Abstract Effects of extramuscular myofascial force transmission on the acute effects of aponeurotomy were studied using finite element modeling and implications of such effects on surgery were discussed. Aponeurotomized EDL muscle of the rat was modeled in two conditions: (1) fully isolated (2) with intact extramuscular connections. The specific goal was to assess the alterations in muscle length-force characteristics in relation to sarcomere length distributions and to investigate how the mechanical mechanism of the intervention is affected if the muscle is not isolated. Major effects of extramuscular myofascial force transmission were shown on muscle length-force characteristics. In contrast to the identical proximal and distal forces of the aponeurotomized isolated muscle, substantial proximo-distal force differences were shown for aponeurotomized muscle with extramuscular connections (for all muscle lengths $F_{dist} > F_{prox}$ after distal muscle lengthening). Proximal optimal length did not change whereas distal optimal length was lower (by 0.5 mm). The optimal forces of the aponeurotomized muscle with extramuscular connections exerted at both proximal and distal tendons were lower than that of isolated muscle (by 15 and 7%, respectively). The length of the gap separating the two cut ends of the intervened aponeurosis decreases substantially due to extramuscular myofascial force transmission. The amplitude of the difference in gap length was muscle length dependent (maximally 11.6% of the gap length of the extramuscularly connected muscle). Extramuscular myofascial force transmission has substantial effects on distributions of lengths of sarcomeres within the muscle fiber populations distal and proximal to the location of intervention: (a) Within the distal population, the substantial sarcomere shortening at the proximal ends of muscle fibers due to the intervention remained unaffected however, extramuscular myofascial force transmission caused a more pronounced serial distribution towards the distal ends of muscle fibers. (b) In contrast, extramuscular myofascial force transmission limits the serial distribution of sarcomere lengths shown for the aponeurotomized isolated muscle in the proximal population. Fiber stress distributions showed that extramuscular myofascial force transmission causes most sarcomeres within the aponeurotomized muscle to attain lengths favorable for higher force exertion. It is concluded that acute effects of aponeurotomy on muscular mechanics are affected greatly by extramuscular myofascial force transmission. Such effects have important implications for the outcome of surgery performed to improve impeded function since muscle in vivo is not isolated both anatomically and mechanically.

Keywords Aponeurotomy · Extramuscular myofascial force transmission · Muscle length-force characteristics · Sarcomere length distributions · Finite element method · Rat extensor digitorum longus (EDL) muscle ·

C. A. Yucesoy (✉)
Biomedical Engineering Institute, Boğaziçi University,
34342, Bebek – Istanbul, Turkey
e-mail: can.yucesoy@boun.edu.tr

C. A. Yucesoy · P. A. Huijing
Instituut voor Fundamentele en Klinische
Bewegingswetenschappen, Faculteit Bewegingswetenschappen,
Vrije Universiteit, Amsterdam, The Netherlands

C. A. Yucesoy · B. H. F. J. M. Koopman · H. J. Grootenboer ·
P. A. Huijing
Integrated Biomedical Engineering for Restoration of Human
Function, Faculteit Constructieve Technische Wetenschappen,
Universiteit Twente, Enschede, The Netherlands

1 Introduction

Contractures occurring in spastic paresis limit the joint range of motion. One of the surgical techniques used to lengthen

such overly short muscles is aponeurotomy (e.g., Baumann and Koch 1989). During this operation the intramuscular aponeurosis is cut transversely, the joint angle is adjusted to lengthen the target muscle and the limb is usually placed in a cast. Recent experiments on rat muscles provided an understanding of the acute (Jaspers et al. 1999, 2002; Brunner et al. 2000) and long term (Brunner et al. 2000) physiological effects of aponeurotomy. These authors reported that below the location of the intervention, isometric lengthening yields progressive rupturing of the intramuscular connective tissue. As a result, muscle length-force characteristics were shown to change substantially.

However, these studies were performed on isolated muscle, whereas in its natural environment of functioning muscle is not isolated. In contrast, it has connections to its surrounding muscles and non-muscular structures. The connections of the extracellular matrix of a muscle to the surrounding non-muscular structures and to bone are referred to as *extramuscular connections*. Such connections include neurovascular tracts in addition to compartmental boundaries comprised of tissues like interosseal membrane and intermuscular septum.

In previous studies, our research groups showed that the extramuscular connections form an important pathway for transmission of force from muscle: *extramuscular myofascial force transmission* (Huijing and Baan 2001; Huijing et al. 2003; Maas et al. 2003; Yucesoy et al. 2003, 2006c). Moreover, adjacent myofibrils are connected and transsarcolemmal proteins connect peripheral myofibrils to the extracellular matrix along the full length of the muscle fiber (for a review see Berthier and Blaineau 1997). These structures were also shown to transmit muscle force: *intramuscular myofascial force transmission* (Huijing 1999). Due to continuity of these force transmission mechanisms, extramuscular myofascial force transmission affects muscular mechanics substantially leading to unequal proximal and distal muscle forces and major alterations in sarcomere length distributions (e.g., Huijing and Baan 2001; Yucesoy et al. 2003).

Finite element method is a powerful technique in studying skeletal muscle mechanics: muscle tissue is considered as a continuum accounting for the material and geometric non-linearities. This method has been applied successfully (e.g., Gielen 1998; van der Linden 1998; Johansson et al. 2000; Oomens et al. 2003). However, use of elements in which both active and passive properties of muscle tissue are lumped is not suitable to study the effects of myofascial force transmission. In order to do that explicitly, we developed a model using a two-domain approach: the intracellular and the extracellular matrix domains of skeletal muscle are represented by two separate but elastically linked meshes (Yucesoy et al. 2002). Using this model, we recently studied the acute effects of aponeurotomy on fully isolated rat muscle and showed that intramuscular myofascial force transmission dominates the acute effects of the intervention (Yucesoy et al. 2006a). Therefore, taking into account the continuity of intra- and extramuscular myofascial structures we hypothesized that the mechanical mechanism of the acute effects of aponeurotomy are altered by extramuscular myofascial force transmission. The goal of the present study is to test this hypothesis using the model of aponeurotomized muscle extended to include extramuscular connections.

2 Methods

2.1 Description of the "linked fiber-matrix mesh model"

In the linked fiber-matrix mesh model (lfmm model), skeletal muscle is considered explicitly as two separate domains: (1) the intracellular domain and (2) extracellular matrix domain. The transsarcolemmal attachments are considered as elastic links between the two domains (Yucesoy et al. 2002).

Two self-programmed elements were developed and were introduced as user-defined elements into the finite element program ANSYS 9.0. One of these elements (*extracellular matrix element*) represents the collagen reinforced extracellular matrix, which includes the basal lamina and connective tissue components such as endomysium, perimysium and epimysium. A second element models the muscle fibers (*myofiber element*). Within the biological context, the combined *muscle element* represents a segment of a bundle of muscle fibers with identical material properties, its connective tissues and the links between them. This is realized as a linked system of extracellular matrix and myofiber elements (for a schematic 2D-representation of an arrangement of these muscle elements see Yucesoy et al. 2002).

In the lfmm model, the extracellular matrix domain is represented by a mesh of extracellular matrix elements (*matrix mesh*). In the same space, a separate mesh of myofiber elements is built to represent the intracellular domain (*fiber mesh*). The two meshes are rigidly connected to single layers of elements modeling proximal and distal aponeuroses: a node representing myotendinous connection sites is the common node of all three (extracellular matrix, myofiber and aponeurosis) elements. In contrast, at the intermediate nodes, fiber and matrix meshes are linked elastically to represent the transmembranous attachments of the cytoskeleton and extracellular matrix. For these links (the model includes a total of 28 of them: 14 in each of the upper and lower model surfaces) the standard element, COMBIN39 is used from the element library of ANSYS 9.0. This is a 2-node spring element, which is set to be uniaxial and have linear high stiffness characteristics representing non-pathological connections between the muscle fibers and the extracellular matrix (for an analysis of the effects of stiff or compliant links, see Yucesoy et al. 2002). Note that at the initial

muscle length and in passive condition, these links have a length equaling zero.

Both extracellular matrix and myofiber elements have eight nodes, linear interpolation functions and a large deformation analysis formulation are applied. A 3D local coordinate system representing the fiber, cross-fiber (normal to the fiber direction), and thickness directions is used. The stress formulation, $\underline{S}$ based on Second Piola–Kirchoff definition constitutes the derivative of the strain energy density function, W with respect to the Green–Lagrange strain tensor, $\underline{L}^G$

$$\underline{S} = \frac{dW}{d\underline{L}^G} \tag{1}$$

2.1.1 Extracellular matrix element

The strain energy density function mechanically characterizing the extracellular matrix includes two parts:

$$W = W_1 + W_2 \tag{2}$$

The first part represents the non-linear and anisotropic material properties (Huyghe et al. 1991):

$$W_1 = W_{ij}(\varepsilon_{ij}) \tag{3}$$

where

$$\begin{aligned} W_{ij}(\varepsilon_{ij}) &= \mathrm{k}.(\mathrm{e}^{\mathrm{a}_{ij}.\varepsilon_{ij}} - \mathrm{a}_{ij}.\varepsilon_{ij}) \quad \text{for } \varepsilon_{ij} > 0 \\ W_{ij}(\varepsilon_{ij}) &= -W_{ij}(|\varepsilon_{ij}|) \quad \text{for } \varepsilon_{ij} < 0 \text{ and } i \neq j \end{aligned} \tag{4}$$

ε_{ij} are the Green–Lagrange strains in the local coordinates. The indices $i = 1, \ldots, 3$ and $j = 1, \ldots, 3$ represent the local cross-fiber, fiber and thickness directions respectively. $\mathrm{a_{ij}}$ and k are constants (Table 1). Note that, initial passive stiffness (k) and passive fiber direction stiffness (a_{22}) values were estimated by fitting the experimental data by Meijer et al. (1996). Based on the experimental data on dog diaphragm (Strumpf et al. 1993), passive cross-fiber stiffness ($a_{11} = a_{33}$) was taken to be higher than fiber direction stiffness. Identical values are used for fiber and fiber-cross fiber shear stiffness ($a_{12} = a_{23} = a_{31}$). However, in contrast to the non-symmetric stress-strain relationships defined for fiber and cross-fiber directions a symmetric stress–strain relationship is used for shearing. The resulting stress–strain curves are shown in Fig. 1a.

The second part includes a penalty function to account for the constancy of muscle volume. The intracellular fluid and solid elastic structures are considered as separate constituents of muscle tissue with different responses to deformation: The intracellular fluid is assumed to have the ability to migrate freely within the cell, whereas, the solid elastic structures housing muscle fibers (e.g., basal lamina and endomysium) are restricted in moving as they are being constrained by neighboring cells. Therefore, a penalty function consisting of two parts was used:

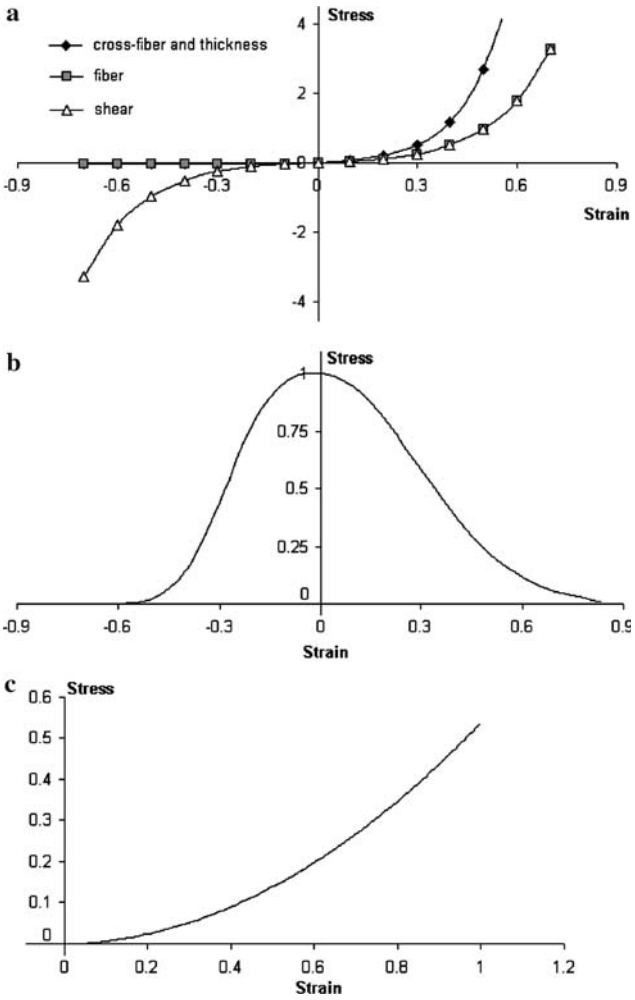


Fig. 1 The stress–strain characteristics of the modeled muscle tissue. **a** Stress (N/mm^2) and strain relationships showing the passive, non-linear and anisotropic mechanical properties of the extracellular matrix element in the local coordinates. **b** Active stress and strain relationship of the myofiber element representing the contractile apparatus. **c** Mechanical properties representing the cytoskeleton of which the titin filaments dominates the passive resistance in the myofiber element. The curves shown in **b** and **c** are normalized for the maximum value of active contractile stress. Note that the active and passive mechanical properties of the myofiber element are valid only for the local fiber direction

$$W_2 = S_s.(I_3 - 1)^2 + S_f.(I_3^{\mathrm{avg}} - 1)^2 \tag{5}$$

where I_3 is the third invariant (determinant) of the Right Cauchy–Green strain tensor providing a ratio of the deformed local volume over the undeformed local volume for each Gaussian point.

If all I_3's are kept as unity, the element is considered as solid and the local volumes are conserved. If the weighted mean of all I_3's per element, (I_3^{avg}) is kept as unity, the element is considered as a fluid. The penalty parameters S_s (for the solid volume) and S_f (for the fluid volume), allow

Table 1 Values and definitions of the model constants

Constant	Value	Unit	Definition
k	0.05	N/mm^2	Initial passive stiffness (Eq. 4)
a_{11}	8.0	–	Passive cross-fiber direction stiffness, $a_{11} = a_{33}$ (Eq. 4)
a_{22}	6.0	–	Passive fiber direction stiffness (Eq. 4)
a_{12}	6.0	–	Passive fiber-cross-fiber shear stiffness, $a_{12} = a_{23} = a_{31}$ (Eq. 4)
S_s	10.0	N/mm^2	Weight factor in the penalty function for the solid volume (Eq. 5)
S_f	80.0	N/mm^2	Weight factor in the penalty function for the fluid volume (Eq. 5)
b_1	30.0	–	Coefficient for the stress–strain relation of the contractile elements (Eq. 6)
b_2	−6.0	–	Coefficient for the stress–strain relation of the contractile elements (Eq. 6)
b_3	1	–	Coefficient for the stress–strain relation of the contractile elements (Eq. 6)
t_1	0.522	–	Coefficient for the stress–strain relation of the intracellular passive elements (Eq. 7)
t_2	0.019	–	Coefficient for the stress–strain relation of the intracellular passive elements (Eq. 7)
t_3	−0.002	–	Coefficient for the stress–strain relation of the intracellular passive elements (Eq. 7)
a_{10}	7.9	N/mm^2	Mooney–Rivlin material constant for aponeurosis elements (Eq. 8)
a_{01}	7.9	N/mm^2	Mooney–Rivlin material constant for aponeurosis elements (Eq. 8)
υ	0.3	–	Poisson's ratio for aponeurosis elements (Eq. 8)

determining the penalty given for each part. Note that if both I_3's and I_3^{avg}'s are unity the volume is constant. The parameters S_s and S_f (Table 1) chosen after performing specific tests on the extracellular matrix element allow a good representation of constancy of muscle volume with optimal numerical efforts: for even very large deformations (e.g., length changes greater than 40%) the maximal deviation from undeformed volume remains below 5%.

2.1.2 Myofiber element

Maximally activated muscle is studied. Sarcomeres within the muscle fibers, are assumed to have identical material properties. The force–velocity characteristics are not considered due to the isometric nature of the present work. The total stress for the intracellular domain (σ_{22f}) is a Cauchy stress acting in the local fiber direction exclusively and is the sum of the active stress of the contractile elements ($\sigma_{22contr}$) and the stress due to intracellular passive tension (σ_{22icp}).

To define the active length–force characteristics, an exponential function (Fig. 1b) was fit to the experimental data of small rat gastrocnemius medialis (GM) fiber bundles (Zuurbier et al. 1995). This function is scaled such that at optimum length, the fiber direction strain (ε_{22}) is zero and the maximal stress value is unity.

$$\begin{aligned} \sigma_{22\text{contr}}(\varepsilon_{22}) &= b_3 e^{b_2 \varepsilon_{22}^3} \quad \text{for } \varepsilon_{22} > 0 \text{ or} \\ \sigma_{22\text{contr}}(\varepsilon_{22}) &= b_3 e^{b_1 \varepsilon_{22}^4} \quad \text{for } \varepsilon_{22} < 0 \end{aligned} \tag{6}$$

where b_1, b_2 and b_3 are constants (Table 1).

The source of intracellular passive tension is the intrasarcomeric cytoskeleton (Trombitas et al. 1995), which is composed of several proteins. In this work titin is considered to play the dominant role. Experimental tension-sarcomere length data (Trombitas et al. 1995) for a single rabbit skeletal muscle fiber was fitted using a parabolic function (Fig. 1c) and scaled to make it compatible to the stress-strain characteristics of the contractile part.

$$\begin{aligned} &\sigma_{22\text{icp}}(\varepsilon_{22}) = t_1 \varepsilon_{22}^2 + t_2 \varepsilon_{22} + t_3 \quad \text{and} \\ &\sigma_{22\text{icp}}(\varepsilon_{22}) = 0 \quad \text{for } \varepsilon_{22} < 0 \end{aligned} \tag{7}$$

where t_1, t_2 and t_3 are constants (Table 1).

2.1.3 Aponeurosis element

To represent the aponeuroses, a standard 3D, 8-node element HYPER58, from the element library of ANSYS 9.0 is used. This element has a hyperelastic mechanical formulation for which the strain energy density function is defined using the two parameter Mooney–Rivlin material law:

$$W = a_{10}(\bar{I}_1 - 3) + a_{01}(\bar{I}_2 - 3) + \frac{\kappa}{2}(\bar{I}_3 - 1)^2 \tag{8}$$

where, $\bar{I}_i i = 1, \ldots, 3$ are reduced invariants of right-Cauchy strain tensor, a_{10} and a_{01} are Mooney–Rivlin material constants, $\kappa = 2(a_{10} + a_{01})/(1 - 2\upsilon)$ is the bulk modulus and υ is the Poisson's ratio. The parameters used (Table 1) ensure sufficient stiffness for the aponeuroses for a representative role in force transmission and providing muscular integrity as in real muscle.

It is assumed that, at the initial muscle length in the passive state, the sarcomeres arranged in series within muscle fibers have identical lengths. Local strain, as a measure of change of length, reflects the lengthening (positive strain) or shortening

(negative strain) of sarcomeres. Note that zero strain in the model represents the undeformed state of sarcomeres (i.e., sarcomere length $\cong$ 2.5 μm) in the passive condition at initial muscle length (28.7 mm). Fiber direction strain within the fiber mesh of the lfmm model was used to assess the non-uniformity of lengths of sarcomeres arranged in-series within muscle fibers (referred to as serial distribution). Muscle length equaling 25.2, 29.2 and 31.2 mm will be referred to as *low muscle length*, *intermediate muscle length* and *high muscle length* respectively.

2.2 Aponeurotomized EDL muscle models

In surgery, after cutting its aponeurosis transversely (Fig. 2a), the muscle is lengthened passively. Experiments on aponeurotomized rat muscle showed that below the location of the intervention, intramuscular connective tissue ruptures in the muscle fiber direction (Fig. 2c) on activation and such effects increase progressively after isometric activity at higher muscle length (Jaspers et al. 1999). Presumably in human patients, further rupturing occurs on activation of the immobilized muscle after the actual operation.

Extensor digitorum longus (EDL) muscle of the rat was modeled. This muscle has a relatively simple geometry: it is a unipennate muscle with rather small pennation angles and minimal variation of the fiber direction within the muscle belly. The geometry of the model (Fig. 2b) is defined as the contour of a longitudinal slice at the middle of the isolated rat EDL muscle belly. Three muscle elements in series and six in parallel fill this slice. Therefore, any collection of three muscle elements arranged in series represents a big muscle fascicle. All aponeurosis elements have identical mechanical properties but using a variable thickness in the fiber-cross fiber plane, the increasing cross-sectional area of the aponeurosis toward the tendon (Zuurbier et al. 1994) is accounted for.

The effects of proximal aponeurotomy were modeled by disconnecting the common nodes of two neighboring aponeurosis elements in the middle of the proximal aponeurosis as well as the two parallel arranged muscle elements located below it (Fig. 2b). As a consequence of the rupture, a wide gap opens between the cut ends of the aponeurosis. However, in the model the tear depth is limited by the length of these proximal muscle elements in the fiber direction. Figure 2d shows the typical deformed shape of the modeled aponeurotomized EDL muscle after distal lengthening and illustrates these features.

Aponeurotomized EDL muscle was studied in two conditions:

(1) Fully isolated. This muscle is referred to as aponeurotomized isolated muscle (*AT isolated*).

(2) With intact extramuscular connections. This muscle is referred to as aponeurotomized muscle with extramuscular connections (*AT extramuscularly connected*).
An extramuscular connective tissue connects EDL all along the muscle to the tibia, part of interosseal membrane and anterior intermuscular septum (Fig. 3a). Under conditions of unphysiological loading this structure is seen as a sheet (for images see Huijing and Baan 2001; Maas et al. 2001). This structure defines the anatomical path of extramuscular myofascial force transmission. In our previous experimental study (Yucesoy et al. 2003), the locations of the extramuscular connections to EDL muscle were determined to be predominantly at one-third of the fascicle length from the most proximal end of each muscle fascicle. In that study it was also shown that the extramuscular connective tissues supporting the major neural and vascular branches supplying the EDL muscle proximally, are much stiffer than the distal of the connective tissue structure.

In order to model the muscles' extramuscular connections and to account for their continuity with the muscular extracellular matrix, a set of nodes of the matrix mesh were linked using spring elements (COMBIN39, from the element library of ANSYS 9.0) to a set of fixed points (Fig. 3b). Our modeling considerations were: (1) the set of fixed points comprising "mechanical ground" represent bone, which is assumed to be rigid. (2) the spring elements modeling the muscles' extramuscular connections were set to be uniaxial and have linear length-force characteristics. (3) Initially (i.e., muscle length = 28.7 mm, and before changing any of the tendon positions), the fixed points and the corresponding nodes of the model were at identical locations (i.e., the spring elements modeling the muscles' extramuscular connections were at a length of zero). (4) The higher stiffness of the connective tissues constituting the neurovascular tract near the EDL muscle is taken into account by making the three most proximal links to the muscle stiffer than distal ones. Stiffness values determined previously (Yucesoy et al. 2003) were used (i.e., k = 0.286 unit force/mm for stiffer part and, k = 0.067 unit force/mm for the more distal links).

2.3 Solution procedure

The analysis type used in ANSYS was static and large strain effects were included. During the entire solution procedure, the models studied were stable and no mesh refinement was performed. A force based convergence criterion was used with a tolerance of 0.5%.

Initially, at the passive state, the activation coefficient b_3 (Eq. 6) equaled 0. Maximal activation of the muscles

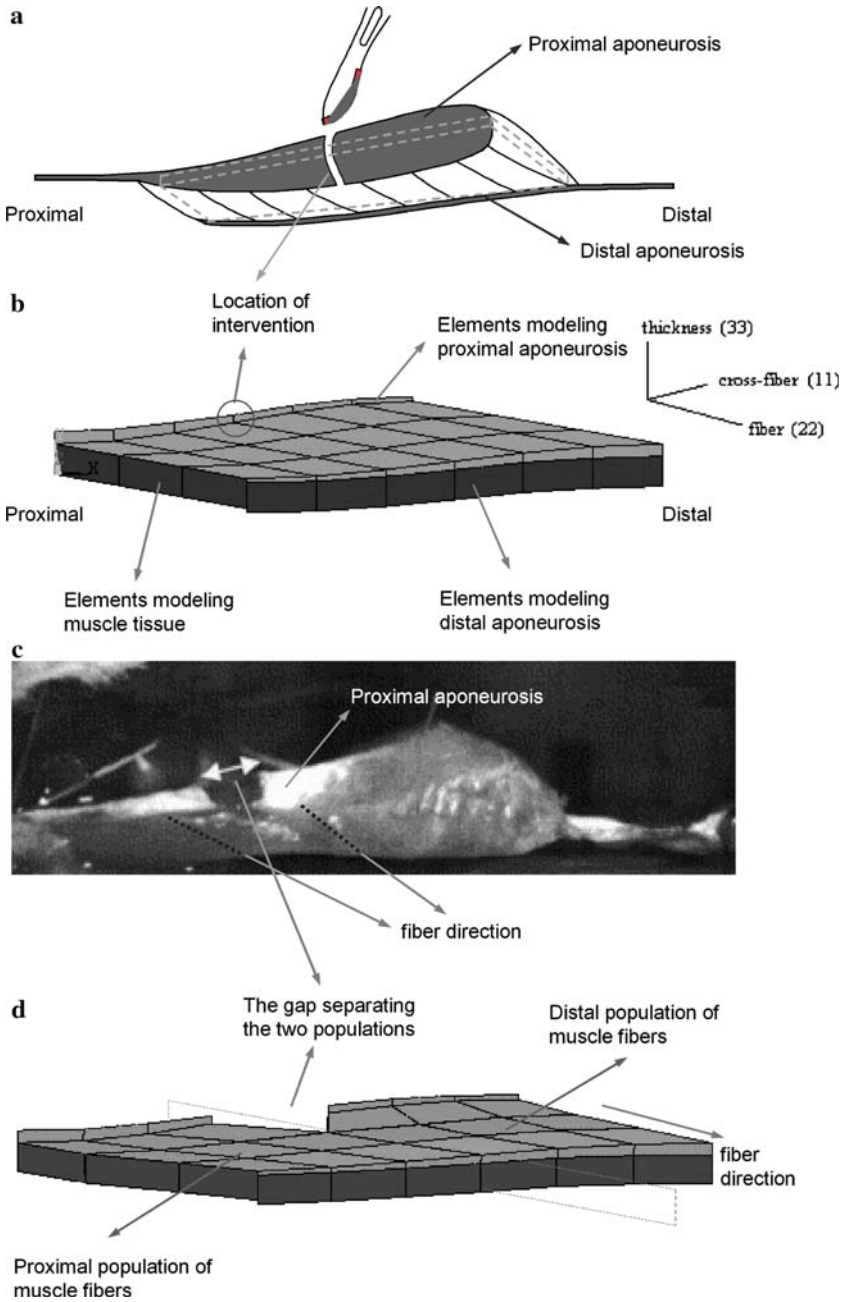


Fig. 2 Finite element modeling of EDL muscle and the acute effects of aponeurotomy. **a** The nature of aponeurotomy shown schematically on rat gastrocnemius muscle. Surgical aponeurotomy as described by Baumann and Koch (1989) involves at least limited fasciotomy followed by one or multiple incisions in the aponeurosis of the target muscle. The incisions are made transversely i.e., in the direction perpendicular to the longitudinal direction of aponeurosis. *Dashed lines* illustrate the modeled longitudinal muscle slice at the middle of the muscle belly. **b** The model of isolated EDL muscle. The model consists of three muscle elements in series and six in parallel. The muscle elements located proximally and distally are connected to elements representing the muscles' aponeuroses. A 3D local coordinate system representing the fiber, cross-fiber (normal to the fiber direction), and thickness directions is used for the analysis and presentation of the model results. The nodes at the upper face of the model (marked by a *circle*) indicate the location of intervention modeled. Proximal aponeurotomy is modeled by disconnecting the common nodes of two neighboring aponeurosis elements located in the middle of the proximal aponeurosis of the modeled muscle. Note that the nodes at the same location of the lower face of the model are also disconnected. **c** Tearing of the intramuscular connective tissues of active muscle after aponeurotomy. Such tearing causes a gap to open between the cut ends of the aponeurosis. The image showing aponeurotomized GM muscle of the rat in situ is redrawn after Jaspers et al. (1999). **d** Typical deformed shape of modeled proximally aponeurotomized muscle after distal lengthening. The gap between the disconnected ends of the aponeurosis creates two distinct populations of muscle fibers that are referred to as "proximal population" and "distal population". The plane marked by *dotted lines* shows the interface between the two populations

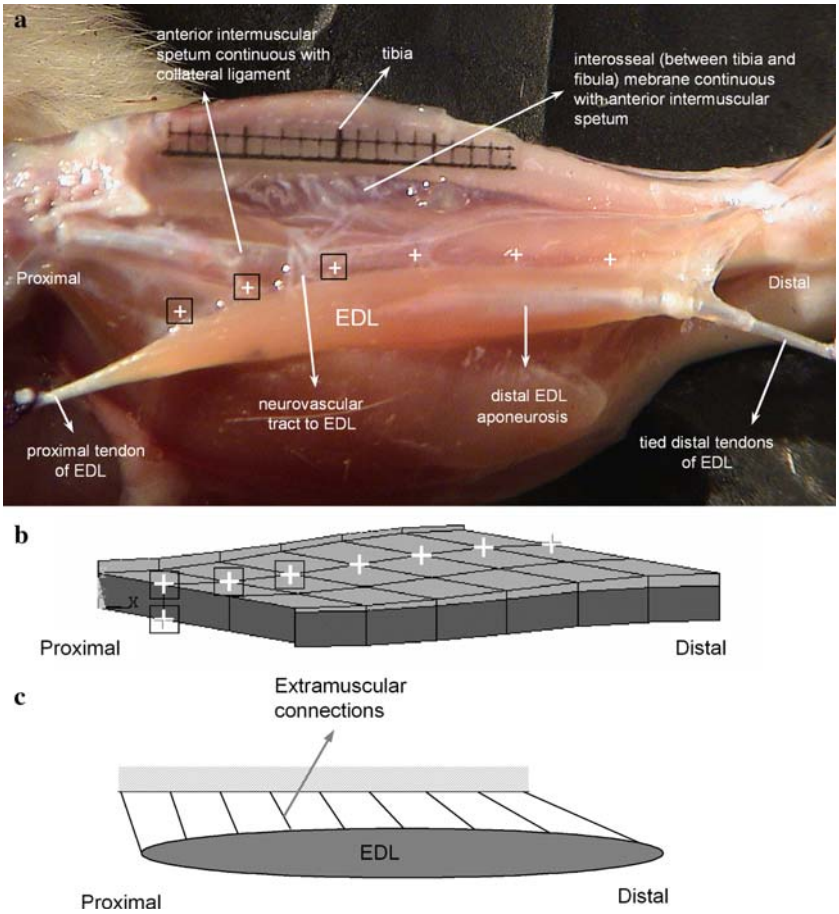


Fig. 3 Extramuscular connections of EDL muscle of the rat and finite element modeling of extramuscularly connected muscle. **a** Rat EDL muscle and its extramuscular connections. The neurovascular tract (i.e., the connective tissue structure embedding nerves and blood vessels, marked by *white* +) is continuous with the interosseal membrane, anterior crural fascia (not shown) and lateral collateral ligament providing connections for EDL muscle to bone all along the muscle belly. Such integral system of connective tissues comprises the pathway of extramuscular myofascial force transmission and provides connections to bone in addition to myotendinous connections to muscle origin and insertion. The part of this tract marked also by a black square show the stiffer proximal segment of extramuscular connections. Note that in order to show the extramuscular connective tissues clearly, a non-physiological, but identical, downward force is exerted on both proximal and distal tendons of EDL moving the muscle from its natural position. **b** The model of EDL muscle with extramuscular connections. The nodes of the matrix mesh marked by a *white* "+" sign have extramuscular connections to mechanical ground and the nodes marked also by a *black square* have stiffer connections. **c** Schematic representation of the effects of changes of muscle relative position on the muscles' extramuscular connections. Due to distal lengthening, at higher muscle lengths these connections are stretched causing a proximally directed load to act on the muscle. Such loads are integrated in distally exerted muscle force and and are responsible for the proximo-distal force differences calculated to favor of muscle distal force. Note that mechanical ground to which the extramuscular connections are connected represent the bone which is assumed as rigid

modeled was achieved by increasing b_3 incrementally up to 1, using fixed increments.

Subsequent to activation, the proximal end of aponeurotomized muscle with extramuscular connections was displaced distally by 2 mm and fixed. The position of proximal end of aponeurotomized isolated muscle was then kept constant during the entire modeling. For both muscles, muscle length was altered by changing the position of muscle distal tendon: first in proximal direction (i.e., to shorten the muscle) then in distal direction (i.e. to lengthen the muscle). For the extramuscularly connected muscle, Fig. 3c illustrates the effects of such changes of muscle position on the extramuscular connections of the muscle at high muscle length.

3 Results

3.1 Effects of extramuscular myofascial force transmission on length-force characteristics of aponeurotomized muscle

Identical forces are exerted at proximal and distal tendons of the aponeurotomized isolated muscle. In contrast, a major

effect of extramuscular myofascial force transmission on muscle force is a substantial proximo-distal force difference: after distal lengthening, EDL distal active forces are higher than proximal forces at all muscle lengths studied (Fig. 4).

Comparing active length-force characteristics of the modeled aponeurotomized muscles shows that the proximal optimum length of aponeurotomized muscle with extramuscular connections is identical to the optimum length of aponeurotomized isolated muscle (30.7 mm). However, the distal optimum length of extramuscularly connected muscle is lower (by 0.5 mm). In addition, the optimal force for the isolated muscle is higher than that of extramuscularly connected muscle both proximally and distally: for extramuscularly connected muscle, proximal optimal force is 85 % and distal optimal force is 93 % of that of isolated muscle (Fig. 4).

The aponeurotomized muscle with extramuscular connections also shows proximo-distal differences in passive forces. This difference also favors the distal force. Note that, the distal passive forces start increasing at much lower muscle lengths than proximal passive forces. This indicates that the proximal end of the passive muscle remains slack even at higher muscle lengths (<30 mm), despite the fact that distal force is exerted.

We conclude that extramuscular myofascial force transmission has sizable effects on muscle length-force characteristics of the aponeurotomized muscle. Such effects are characterized primarily by variable proximo-distal force differences. However, adding extramuscular connections did not cause additional muscle lengthening as an effect of aponeurotomy. Nevertheless, the differences in length-force characteristics indicate that extramuscular myofascial force transmission modifies the effects of aponeurotomy on distributions of sarcomere lengths.

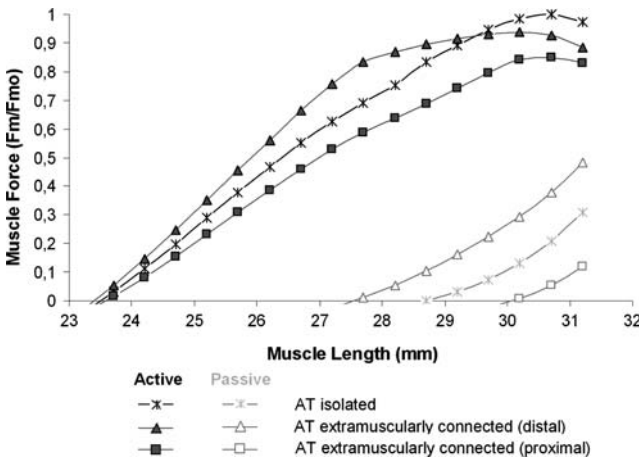


Fig. 4 The isometric muscle length-force curves of modeled aponeurotomized EDL muscles. Active and passive isometric forces of aponeurotomized (*AT*) isolated muscle and aponeurotomized muscle with extramuscular connections are compared. Note that the forces of aponeurotomized isolated muscle exerted at the proximal and distal ends are identical whereas due to extramuscular myofascial force transmission, the proximal and distal forces of aponeurotomized muscle with extramuscular connections are unequal. Both sets of data are normalized for optimum force of aponeurotomized isolated muscle

3.2 Effects of extramuscular myofascial force transmission on geometry of aponeurotomized muscle and sarcomere length distributions

Figure 5 shows distributions of fiber direction strain, as well as the deformed geometry of the aponeurotomized muscles at three different muscle lengths. For both isolated (Fig. 5a–c) and extramuscularly connected (Fig. 5d–f) muscles, in general, the intervention leads to a gap of increasing length with muscle lengthening separating the two cut ends of the aponeurosis. Tearing of intramuscular connective tissue below the gap causes substantial differences in sarcomere length distributions of the proximal population of muscle fibers (with intact myotendinous junctions at both ends) and the distal population of muscle fibers (lacking myotendinous connection to the muscles' origin). Both aponeurotomized muscles show extreme length changes for the sarcomeres at the proximal ends of the muscle fibers that are connected to either of the cut ends of the proximal aponeurosis.

It should be noted that extramuscular myofascial force transmission modifies the effects of aponeurotomy:

(1) For all muscle lengths the gap length for aponeurotomized muscle with extramuscular connections is substantially smaller than that of aponeurotomized isolated muscle. Note, however, that the amplitude of difference in the gap length between the aponeurotomized muscles is also length dependent (Fig. 6). At the lowest length studied, the difference is 8.3% of the gap length of aponeurotomized muscle with extramuscular connections. This increases up to 11.6% (at muscle length = 27.7 mm). Over this length the difference decreases and is reduced to 5.8% at the highest length studied.

(2) Extramuscular myofascial force transmission limits extreme sarcomere length changes near the cut end of the proximal aponeurosis in the proximal population. For example at intermediate muscle length, sarcomere length change at this location reaches up to +56% for aponeurotomized isolated muscle (Fig. 5b), whereas it is limited to +43% for aponeurotomized muscle with extramuscular connections (Fig. 5e).

(3) Extramuscular myofascial force transmission modifies substantially the distributions of sarcomere lengths in both proximal and distal populations of muscle fibers within the aponeurotomized muscle. Figure 7 in which the two populations of muscle fibers are distinguished shows a detailed comparison between the fiber

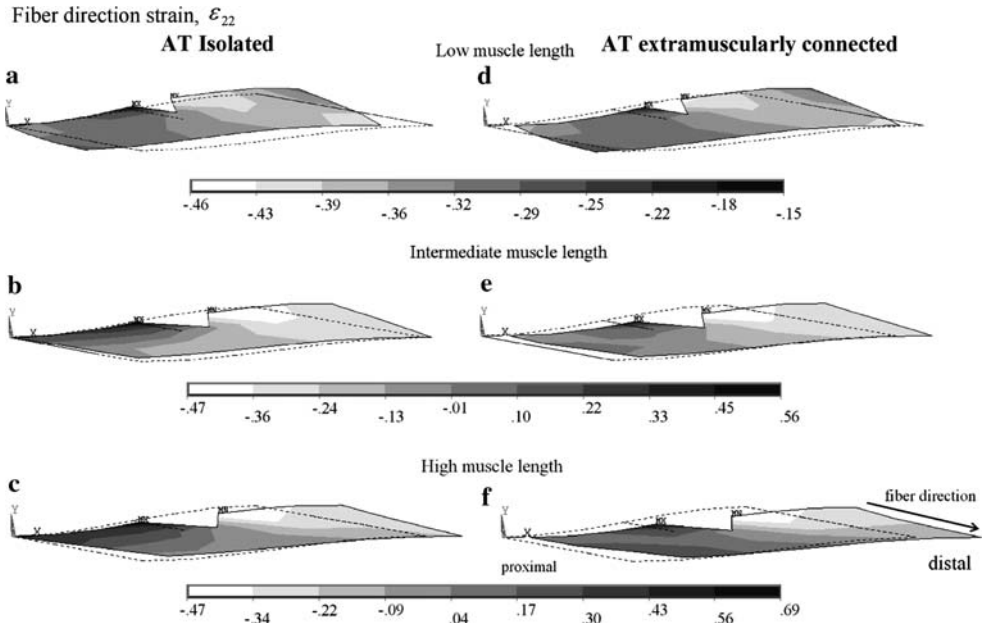


Fig. 5 Fiber direction strains within modeled aponeurotomized isolated muscle and within aponeurotomized muscle with extramuscular connections. *Left panel* The strain distributions within the fiber mesh of active aponeurotomized (*AT*) isolated muscle. *Right panel* The strain distributions within the fiber mesh of active aponeurotomized muscle with extramuscular connections. The location of the intervention was at the middle of the proximal aponeurosis. *Contour plots* are shown for low muscle length (25.2 mm, i.e., **a**, **d**), intermediate muscle length (29.2 mm, i.e., **b**, **e**) and high muscle length (31.2 mm, i.e., **e**, **f**). The dotted line contour indicates passive muscle geometry at the initial length. The local fiber direction as well as the proximal and distal ends of the muscle are indicated (**f**)

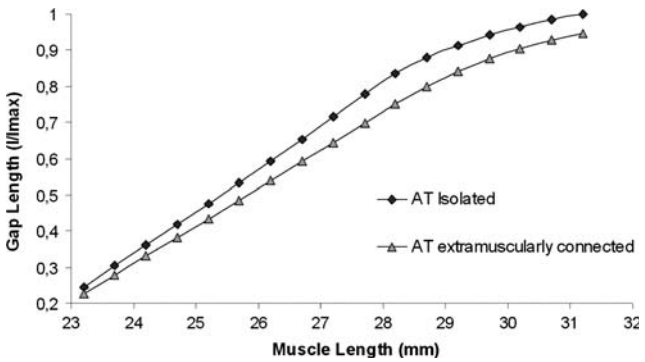


Fig. 6 Length of the gap within the EDL proximal aponeurosis as a function of muscle length. Both sets of data are normalized for maximum gap length of aponeurotomized isolated muscle

direction strain distributions of aponeurotomized isolated muscle and aponeurotomized muscle with extramuscular connections.

Proximal population of muscle fibers: Extramuscular myofascial force transmission limits the serial distributions of sarcomere lengths in the proximal population. This occurs because extramuscular myofascial force transmission leads to two different effects:

(i) In the proximal fascicle sections (Sections I and II) the sarcomeres of the aponeurotomized muscle with extramuscular connections are much shorter. For example, at high muscle length, sarcomere length change in section I varies from +37 to +44% in isolated muscle (Fig. 7c) but only ranges between 0 and +26% for extramuscularly connected muscle (Fig. 7f). Also for fascicle Section II, sarcomere length change varies between +8 and +32% in the isolated muscle (Fig. 7c) whereas, it is limited to values ranging from +3 to +22% in extramuscularly connected muscle (Fig. 7f).

(ii) In contrast, in the distal fascicle sections (Sections III and IV) the sarcomeres of the aponeurotomized muscle with extramuscular connections are much longer than those in the isolated muscle, which effect becomes more pronounced at higher muscle lengths. At high muscle length, within fascicle section III, sarcomeres of extramuscularly connected aponeurotomized muscle are lengthened by 0% up to +31% (Fig. 7f), whereas sarcomere length changes range between −5% (i.e., shortening) to only +9% (i.e., lengthening) for isolated muscle (Fig. 7c). Similarly, but in contrast to the minimal changes in sarcomere lengths shown for fascicle section IV in isolated muscle, sarcomere lengthening reaches values between +7 and +17% in extramuscularly connected muscle.

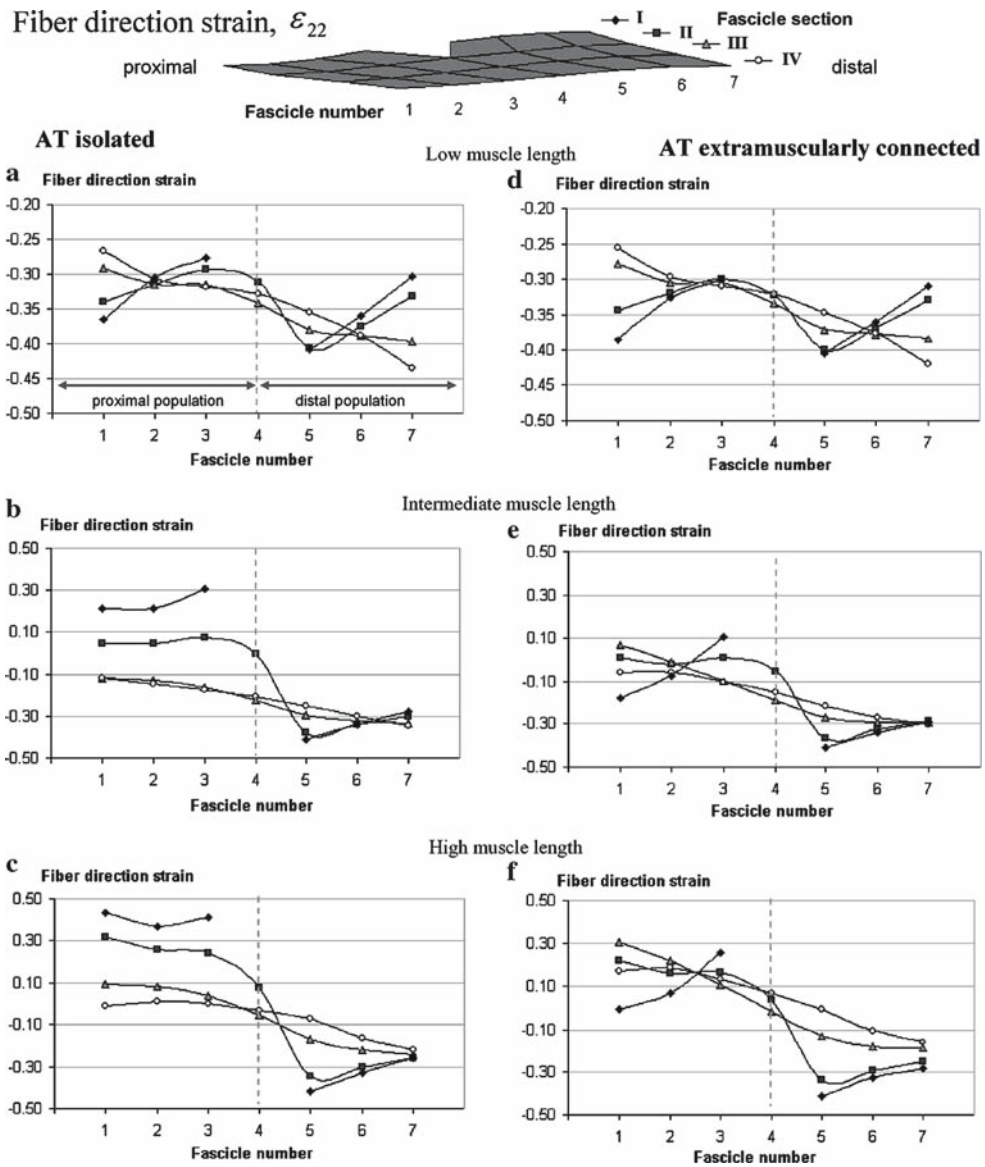


Fig. 7 Detailed analysis of fiber direction strain distribution within modeled aponeurotomized EDL muscles at selected muscle lengths. For four fascicle sections, the nodal fiber direction strains are plotted as a function of fascicle number. Each fascicle is indicated by a number from 1 to 7 and each fascicle section is indicated by a Roman numeral from I to IV (*upper panel*). Differences of strain between sections arranged in series within a fascicle are a measure of the serial distribution of lengths of sarcomeres. *Left panel* The strain distributions within the fiber mesh of active aponeurotomized (*AT*) isolated muscle. *Right panel* The strain distributions within the fiber mesh of active aponeurotomized muscle with extramuscular connections. Strain plots are shown for low muscle length (25.2 mm, i.e., **a**, **d**), intermediate muscle length (29.2 mm, i.e., **b**, **e**) and high muscle length (31.2 mm, i.e., **e**, **f**). The strain distributions in the proximal and distal populations of muscle fibers in both muscles are considered separately. Note that the extreme length changes calculated for the sarcomeres located at the cut ends of the proximal aponeurosis (i.e., the strain values for the nodes located in fascicle section I of fascicle 4) are not shown in this figure

Distal population of muscle fibers: The dominant effect of aponeurotomy, characterized by substantially shortened sarcomeres at the proximal ends of muscle fibers (near the tear), is not affected by extramuscular myofascial force transmission: hardly any differences in sarcomere lengths are found among the proximal fascicle sections (Sections I and II) of isolated and extramuscularly connected muscles for the muscle lengths studied (Fig. 7). However, as a function of muscle lengthening, the sarcomeres found in the distal fascicle sections (Sections III and IV) attain higher lengths as a result of extramuscular myofascial force transmission. For example, at high muscle length sarcomeres in fascicle section III and IV of the extramuscularly connected muscle are minimally +23 and +27% longer respectively, than the

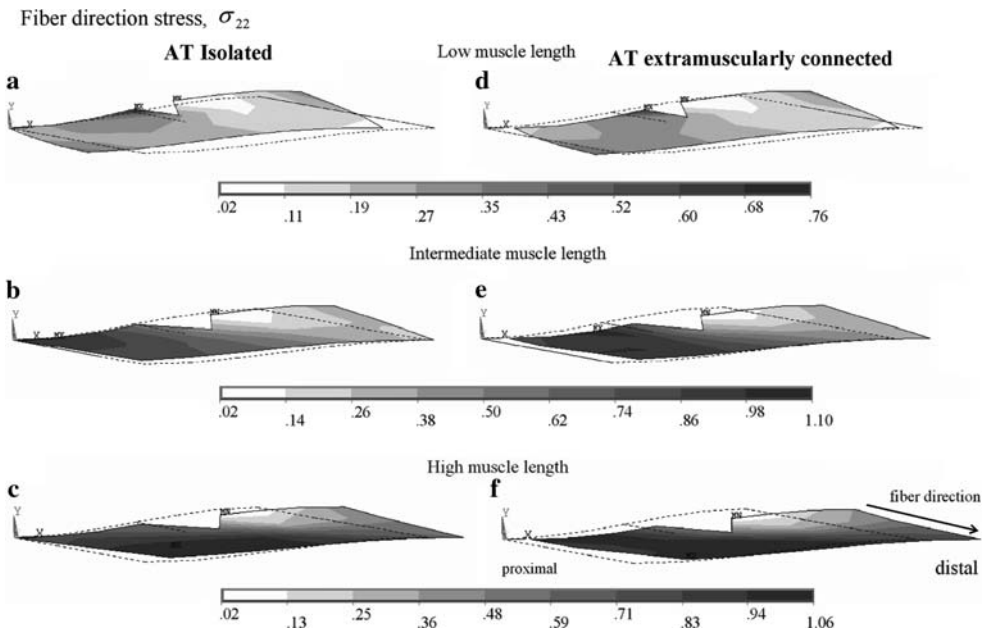


Fig. 8 Fiber direction stress within modeled aponeurotomized isolated muscle and within aponeurotomized muscle with extramuscular connections. *Left panel* The stress distributions within the fiber mesh of active aponeurotomized isolated muscle. *Right panel* The stress distributions within the fiber mesh of active aponeurotomized muscle with extramuscular connections. *Contour plots* are shown for low muscle length (25.2 mm, i.e., **a**, **d**), intermediate muscle length (29.2 mm, i.e., **b**, **e**) and high muscle length (31.2 mm, i.e., **e**, **f**). The *dotted line* contour indicates muscle geometry at the initial length. The local fiber direction as well as the proximal and distal ends of the muscle are indicated (**f**)

sarcomeres located in the corresponding parts of the isolated muscle (Fig. 7c, f). Therefore, in the distal population of muscle fibers extramuscular myofascial force transmission enhances the effects of aponeurotomy leading to a more pronounced serial distribution.

We conclude that extramuscular myofascial force transmission reduces largely the gap length within the aponeurosis and it has substantial effects on distributions of lengths of sarcomeres in aponeurotomized muscle. A remarkable effect is that extramuscular myofascial force transmission effectively limits the substantial lengthening of sarcomeres shown for the proximal population of aponeurotomized isolated muscle.

3.3 Effects of extramuscular myofascial force transmission on fiber direction stress distributions

Stress distributions within the fiber mesh indicate the contribution of sarcomeres at different locations within the aponeurotomized muscle to active muscle force. Figure 8 shows the sizable effects of extramuscular myofascial force transmission on the fiber direction stresses:

(i) Differential effects are found for the proximal and distal populations of muscle fibers. For the proximal population of muscle fibers, extramuscular myofascial force transmission limits the stress distribution found after aponeurotomy. This effect becomes more pronounced as the muscle attains higher lengths. For example at the highest length studied, the stress values show a clear serial distribution ranging between 0.7 and 1.04 in the isolated muscle (Fig. 8c) whereas for a large number of muscle fibers stress approximates unity homogeneously along the entire fiber length in the extramuscularly connected muscle (Fig. 8f).
In contrast to the proximal population of muscle fibers, for the distal population, extramuscular myofascial force transmission enhances the inhomogeneity of the stress values. For example at high muscle length, for the most distal muscle fibers the stress values vary between 0.48 and 0.59 for the isolated muscle (Fig. 8c) and between 0.36 and 0.75 for the extramuscularly connected muscle (Fig. 8f).

(ii) In general, fiber direction stress values calculated for the majority of sarcomeres of the aponeurotomized muscle with extramuscular connections are considerably higher than those calculated for the sarcomeres of the aponeurotomized isolated muscle.

We conclude that extramuscular myofascial force transmission causes most sarcomeres within the aponeurotomized muscle to attain lengths favorable for higher force exertion.

4 Discussion

4.1 Effects of extramuscular myofascial force transmission on the acute effects of aponeurotomy

4.1.1 Proximo-distal force differences

Our present model results show that a major effect of extramuscular myofascial force transmission on aponeurotomized muscle is a substantial proximo-distal force difference. Earlier experiments investigating the effects of aponeurotomy on rat muscles were performed exclusively on fully dissected muscle in situ (Jaspers et al. 1999; Brunner et al. 2000). Therefore, no experimental evidence that shows proximo-distal force differences for aponeurotomized muscle with intact extramuscular connections is available. However, studies of our research groups on intact rat muscles provided substantial evidence on the effects of extramuscular myofascial force transmission including major proximo-distal force differences. Similar to our present results, force differences favoring the distal EDL force were measured after distal lengthening (Huijing and Baan 2001; Yucesoy et al. 2003). In contrast, proximal EDL lengthening caused higher proximal forces (Huijing and Baan 2001). Substantial proximo-distal force differences were shown also for active EDL muscle with epimuscular connections (i.e., the integral system of inter- and extramuscular connections). The length of active EDL muscle was kept constant whereas, (1) the lengths of the active synergistic tibialis anterior (TA) and extensor hallucis longus (EHL) muscles (Maas et al. 2001) or that of active EHL muscle exclusively (Yucesoy et al. 2006b) were manipulated (2) the relative position of active EDL muscle with respect to nonmuscular tissues (Maas et al. 2003; Yucesoy et al. 2006b), as well as both muscular and nonmuscular tissues (Maas et al. 2004) were altered to yield unequal proximal and distal forces. Therefore, the proximo-distal force differences are a consequence of epimuscular myofascial force transmission from the muscle and such force differences shown presently for the aponeurotomized muscle modeled with intact extramuscular connections are likely to occur also experimentally.

Proximo-distal force differences are shown also for passive forces. Note that distal passive forces start building up already at lengths lower than muscle optimum length. This is because the muscles' extramuscular connections represent a certain mechanical load on the muscle opposing lengthening at those relatively low lengths. In our recent experiments, the passive forces of EHL muscle with epimuscular connections were measured to be nonzero for all muscle lengths (Yucesoy et al. 2005). This showed that such tissues within the anterior crural compartment of the rat are prestrained, conceivably due to the prestrain in structures such as the anterior intermuscular septum and interosseal membrane. New studies are needed to determine specifically the mechanical properties of these tissues. However, these findings indicate that the extramuscular myofascial force transmission pathways are sufficiently stiff suggesting that such force transmission may be effective also in vivo.

To resolve problems of movement range, aponeurotomy is a surgical technique applied frequently to bi-articular muscles such as GM (Baumann and Koch 1989) and hamstrings (Reimers 1990; Dhawlikar et al. 1992; Zwick et al. 2002) of patients suffering from spastic paresis. For such muscles, proximo-distal muscle force differences imply asymmetric effects of the operation on the proximal and distal joints that the operated muscle crosses. Our present results suggest that after distal lengthening of aponeurotomized EDL muscle (which is bi-articular in the rat), the contribution of this muscle to the moment exerted at the proximal joint decreases due to extramuscular myofascial force transmission. Therefore, while intending to correct a functional problem at a distal joint, the surgery is likely to alter the mechanics at the proximal joint. Such altered mechanics may also cause unfavorable results. For example, in cerebral palsy, surgical correction of hamstring contractures is performed also in the presence of hip flexor tightness (e.g., Zwick et al. 2002). Aponeurotomy of the semimembranosus in addition to tendon lengthening of the gracilis (by z-plasty) allows increased length range of force exertion distally. However, as indicated by our present results, this may lead to a weakening in hip extension, which effect is contradictory to the additional purpose of correcting hip flexor tightness. Commonly, in this combined functional deficiency lengthening of psoas muscle is performed as well. It is therefore conceivable that this step of such multilevel surgery actually also serves the purpose of counteracting unfavorable effects of the preceding steps. We suggest that especially when operating bi-articular muscles the proximo-distal force differences caused by extramuscular myofascial force transmission should be taken into account.

4.1.2 Length of the gap within the EDL proximal aponeurosis

Earlier experiments on isolated rat GM (Jaspers et al. 1999) and EDL (Jaspers et al. 2002) showed that acutely, aponeurotomy causes (due to rupturing of intramuscular connective tissues along the muscle fiber direction below the location of intervention) a major change in muscle geometry. This change can be characterized by the length of the gap within the muscles' proximal aponeurosis. Our recent modeling work (Yucesoy et al. 2006a) showed that if no such gap is allowed to occur (i.e., the aponeurosis is cut, but the intramuscular connective tissues remain intact) the effects of the intervention are unimportant. Therefore, the dominant mechanism of the effects of the surgery is interfering with the intramuscular myofascial force transmission

mechanism. However, our present results show that extramuscular myofascial force transmission limits the length of the gap, and therefore the changes in muscle geometry. The modifications of sarcomere length distributions within the aponeurotomized muscle are explained by this effect.

4.1.3 Sarcomere length distributions

With aponeurotomy, lengthening of the muscle is intended in order to restore a more normal joint range of motion, if restrictive muscle contractures are caused by for example cerebral palsy. Experiments on fully dissected rat muscles in situ showed that the intervention yields a net increase in the length range of active force exertion due to a shift in muscle optimum length to a higher muscle length (Jaspers et al. 1999; Brunner et al. 2000). For truly isolated EDL muscle, present results and previous modeling (Yucesoy et al. 2006a) show that aponeurotomy acutely leads to major inhomogeneities of lengths of sarcomeres. This explains the shift in muscle optimum length to higher lengths. In dissected muscle with no surgical aponeurotomy, serial sarcomere length distribution (Wohlfart et al. 1977; Morgan et al. 2000) and heterogeneity of mean sarcomere length of different fibers (Willems and Huijing 1994; Huijing et al. 1998) were shown to enhance the muscle length range of active force exertion.

However, for the aponeurotomized muscle with intact extramuscular connections our present results show that the sarcomere length distributions are modified: (1) In the distal population of muscle fibers no notable change in sarcomere lengths occurs within the proximal fascicle sections, whereas, sarcomeres in the distal fascicle sections became longer. This increases the force exerted by sarcomeres located distally however, it does not change sarcomere length inhomogeneity notably. (2) In contrast, for the proximal population of muscle fibers extramuscular myofascial force transmission limits both lengthening of the sarcomeres within the proximal fascicle sections and shortening of the sarcomeres within the distal fascicle sections. This leads to a considerably lower distribution of sarcomere lengths and explains the reduced length range of distal force exertion of the extramuscularly connected aponeurotomized muscle.

Another goal of the surgery, is weakening of the agonist muscle (i.e., reducing muscle force) if an imbalance of antagonistic muscle force is judged to restrict joint motion. Acute substantial reductions of muscle active force for all muscle lengths was reported for the experimented isolated rat muscles (Jaspers et al. 1999; Brunner et al. 2000).

Finite element model results showed for isolated muscle that the dominance of short sarcomeres within the distal fiber population is the major reason for the reduction of muscle active force (Yucesoy et al. 2006a). However, presently we show that changes in sarcomere length distributions caused by extramuscular myofascial force transmission for both proximal and distal populations of muscle fibers allow most sarcomeres within the muscle to attain lengths favorable for exertion of higher active force. This is contradictory to the goal of weakening the muscle.

Despite this effect, it should be noted that at higher muscle lengths (i.e., over 29.7 mm), active distal force of aponeurotomized muscle with extramuscular connections is lower than the active force of aponeurotomized isolated muscle. This is explained by the very high passive forces exerted at the distal tendon (Fig. 4).

We conclude that extramuscular myofascial force transmission alters the sarcomere length distributions in such a way that the clinically intended acute effects of the intervention are limited. Therefore, it is conceivable that dissecting the extramuscular connections of the targeted muscle in addition to transaction of its aponeurosis may allow the *acute* effects to be more pronounced.

4.2 Limitations and implications of the present study

The rupturing of the muscular connective tissue due to aponeurotomy occurs progressively as a function of increasing length (e.g., Jaspers et al. 1999). However, independent of muscle length the modeled tear depth equals the length of the most proximal muscle elements. Therefore, the progressive nature of rupturing is not represented. Nevertheless, our present modeling represents the stabilized tear depth shown to occur experimentally after repeated measurements of muscle length–force characteristics (Jaspers et al. 1999, 2002). Moreover, the present results show that extramuscular myofascial force transmission limits the length of gap within the interfered aponeurosis. This suggests that in surgical practice, the tear within the extramuscularly connected aponeurotomized muscle may be less deep than expected on the basis of experiments on dissected in situ muscle and that these connections may assist controlling of such depth.

The mechanical properties of the modeled EDL muscle and its extramuscular connections represent those of healthy muscle. Although not shown univocally, several studies suggested differences between spastic and healthy muscle. Spastic muscles (e.g., Tardieu et al. 1982; Sinkjaer and Magnussen 1994) and isolated single muscle fiber segments (Friden and Lieber 2003) were reported to be stiffer than normal. In contrast, Lieber et al. (2003) showed for passive bundles muscle fibers that despite being hypertropic the collagen reinforced extracellular matrix of spastic muscle tissue was less stiff. Conceivably, if the intramuscular connective tissues are stiffer than presently modeled, more resistance to sarcomere shortening is expected. This may alter the effects (e.g., a less pronounced effect in the distal population of muscle fibers). On the other hand, it is also likely that the extramuscular connections of the muscle are stiffer than those of healthy muscle. Such stiffer extramuscular connections may even be

involved in the etiology of restricted joint motion (Smeulders 2004). This needs to be studied.

In spastic muscle, limiting either the lengthening of muscle fibers or the rate of such lengthening is expected to lead to limited receptor activity of muscle spindles. Aponeurotomy was reported to contribute to such limiting effects and therefore to decreasing the degree of muscle spasticity (e.g., Suso et al. 1985). Strain distributions in the fiber direction calculated using our model allow for an assessment of such potentially positive effect of the intervention. For the isolated muscle, the dominance of short sarcomeres in the distal population of muscle fibers even at higher muscle lengths indicates reduced strain on the muscle spindles. In contrast, in the proximal population of muscle fibers, sarcomeres within the proximal fascicle section are highly lengthened. However, for extramuscularly connected aponeurotomized muscle, those sarcomeres attain much lower lengths and in general the lengths of sarcomeres within the proximal population vary within a narrower range. Therefore, it is conceivable that extramuscular myofascial force transmission contributes to a reduction of the degree of spasticity of this part of the muscle.

After recovery muscle geometry was shown to be changed again: (1) the continuity of the collagen reinforced extracellular matrix is reestablished (Brunner et al. 2000; Jaspers et al. 2005) and (2) a new connective tissue structure reconnects the cut ends of the aponeurosis (Jaspers et al. 2005). This new tissue was reported to be longer (up to 15%) and more compliant than the regular aponeurotic tissue. These findings suggest that both myotendinous and intramuscular myofascial force transmission paths of the muscle are remodeled, yet the recovered muscle may be longer. If the muscle had been truly isolated, the remodeled force transmission mechanisms should have limited the acute effects of the intervention to a large extent. However, within its natural environment of surrounding connective tissues, sarcomere length inhomogeneity of the healed muscle may increase due to extramuscular myofascial force transmission (Yucesoy et al. 2003, 2005). Therefore, effects of such force transmission may sustain and possibly enhance the lengthening effect of aponeurotomy after recovery.

Our present results imply that aponeurotomy should not be conceived solely as an intramuscular intervention, but the effects of epimuscular myofascial force transmission should also be accounted for. Also for other surgical techniques, major effects of epimuscular myofascial force transmission are conceivable. We will give two supportive examples: (1) In cerebral palsy patients, Kreulen et al. (2003) showed for flexor carpi ulnaris muscle (FCU) that in the neutral wrist position, distal tenotomy caused only a minor shortening of the passive muscle, which hardly increased after a maximal tetanic contraction. However, subsequent dissection of approximately 50% of FCU epimuscular connections did increase muscle shortening on activation substantially. Therefore, such dissection is conceived as the actually effective intervention to limit the contribution of the tenotomized muscle to the joint moment. (2) After transfer surgery of distal tendon of rectus femoris (RF) muscle to a knee flexor position (Delp et al. 1994) RF was shown to still exert a knee extension moment when stimulated (Riewald and Delp 1997) and move in vivo in the same direction as the knee extensors (Asakawa et al. 2002). We suggest that although the muscles' distal tendon is attached to a knee flexor muscle, a substantial fraction of its force is transmitted via epimuscular myofascial pathways onto its synergistic neighbors that still exert a knee extension moment.

In conclusion, our present study shows that the acute effects of aponeurotomy on muscular mechanics are affected seriously by extramuscular myofascial force transmission. Such effects are characterized by (1) proximo-distal force differences suggesting a differential contribution of a bi- or polyarticular muscle to joint moments exerted at the proximal and distal joints. (2) Altered sarcomere length distributions suggesting a limitation to the acute effects of the intervention.

Since muscle in vivo is not isolated anatomically and mechanically, the effects of extramuscular myofascial force transmission have important implications for the outcome of surgery performed to improve impeded function regarding both acute and long term effects.

Acknowledgments This work was supported by (1) Boğaziçi University Research Fund under grant BAP04HX102 to Can A. Yucesoy, (2) the Vrije Universiteit, Amsterdam and (3) the Universiteit Twente, Enschede.

References

Asakawa DS, Blemker SS, Gold GE, Delp SL (2002) In vivo motion of the rectus femoris muscle after tendon transfer surgery. J Biomech 35:1029–1037

Baumann JU, Koch HG (1989) Ventrale aponeurotische Verlängerung des Musculus Gastrocnemius. Oper Orthopaedie Traumatol 1:254–258

Berthier C, Blaineau S (1997) Supramolecular organization of the subsarcolemmal cytoskeleton of adult skeletal muscle fibers. A review. Biol Cell 89:413–434

Brunner R, Jaspers RT, Pel JJ, Huijing PA (2000) Acute and long-term effects on muscle force after intramuscular aponeurotic lengthening. Clin Orthopaed Relat Res 378:264–273

Delp SL, Ringwelski DA, Carroll NC (1994) Transfer of the rectus femoris: effects of transfer site on moment arms about the knee and hip. J Biomech 27:1201–1211

Dhawlikar SH, Root L, Mann RL (1992) Distal lengthening of the hamstrings in patients who have cerebral palsy. Long-term retrospective analysis. J Bone Joint Surg 74:1385–1391

Friden J, Lieber RL (2003) Spastic muscle cells are shorter and stiffer than normal cells. Muscle Nerve 27:157–164

Gielen S (1998) A continuum approach to the mechanics of contracting skeletal muscle. PhD Thesis in Eindhoven University of Technology, Eindhoven, The Netherlands

Huijing PA (1999) Muscular force transmission: a unified, dual or multiple sytem? A review and some explorative experimental results. Arch Physiol Biochem 170:292–311

Huijing PA, Baan GC (2001) Extramuscular myofascial force transmission within the rat anterior tibial compartment: Proximo-distal differences in muscle force. Acta Physiol Scand 173:1–15

Huijing PA, Baan GC, Rebel G (1998) Non myo-tendinous force transmission in rat extensor digitorum longus muscle. J Exp Biol 201:682–691

Huijing PA, Maas H, Baan GC (2003) Compartmental fasciotomy and isolating a muscle from neighboring muscles interfere with extramuscular myofascial force transmission within the rat anterior crural compartment. J Morphol 256:306–321

Huyghe JM, van Campen DH, Arts T, Heethaar RM (1991) The constitutive behaviour of passive heart muscle tissue: a quasi- linear viscoelastic formulation. J Biomech 24:841–849

Jaspers RT, Brunner R, Baan GC, Huijing PA (2002) Acute effects of intramuscular aponeurotomy and tenotomy on multitendoned rat EDL: indications for local adaptation of intramuscular connective tissue. Anat Rec 266:123–135

Jaspers RT, Brunner R, Pel JJM, Huijing PA (1999) Acute effects of intramuscular aponeurotomy on rat GM: Force transmission, muscle force and sarcomere length. J Biomech 32:71–79

Jaspers RT, Brunner R, Riede UN, Huijing PA (2005) Healing of the aponeurosis during recovery from aponeurotomy: morphological and histological adaptation and related changes in mechanical properties. J Orthop Res 23:266–273

Johansson T, Meier P, Blickhan R (2000) A finite-element model for the mechanical analysis of skeletal muscles. J Theor Biol 206:131–149

Kreulen M, Smeulders MJ, Hage JJ, Huijing PA (2003) Biomechanical effects of dissecting flexor carpi ulnaris. J Bone Joint Surg Br 85:856–859

Lieber RL, Runesson E, Einarsson F, Friden J (2003) Inferior mechanical properties of spastic muscle bundles due to hypertrophic but compromised extracellular matrix material. Muscle Nerve 28:464–471

Maas H, Baan GC, Huijing PA (2001) Intermuscular interaction via myofascial force transmission: effects of tibialis anterior and extensor hallucis longus length on force transmission from rat extensor digitorum longus muscle. J Biomech 34:927–940

Maas H, Baan GC, Huijing PA (2004) Muscle force is determined also by muscle relative position: isolated effects. J Biomech 37:99–110

Maas H, Baan GC, Huijing PA, Yucesoy CA, Koopman B HFJM, Grootenboer HJ (2003) The relative position of EDL muscle affects the length of sarcomeres within muscle fibers: experimental results and finite element modeling. J Biomech Eng 125:745–753

Meijer K, Grootenboer HJ, Koopman HFJM, Huijing PA (1996) Isometric length-force curves during and after concentric contractions differ from the initial isometric length-force curve in rat muscle. J Appl Biomech 16:164–181

Morgan DL, Whitehead NP, Wise AK, Gregory JE, Proske U (2000) Tension changes in the cat soleus muscle following slow stretch or shortening of the contracting muscle. J Physiol 522(Pt 3):503–513

Oomens CW, Maenhout M, van Oijen CH, Drost MR, Baaijens, FP (2003) Finite element modelling of contracting skeletal muscle. Philos Trans Roy Soc Lond Ser B Biol Sci 358:1453–1460

Reimers J (1990) Functional changes in the antagonists after lengthening the agonists in cerebral palsy. II. Quadriceps strength before and after distal hamstring lengthening. Clin Orthopaed Relat Res 253:35–37

Riewald SA, Delp SL (1997) The action of the rectus femoris muscle following distal tendon transfer: does it generate knee flexion moment? Dev Med Child Neurol 39:99–105

Sinkjaer T, Magnussen I (1994) Passive, intrinsic and reflex-mediated stiffness in the ankle extensors of hemiparetic patients. Brain 117:355–363

Smeulders MJ (2004) Introducing intraoperative direct measurement of muscle force and myofascial force transmission in tendon transfer for cerebral palsy. PhD Thesis in Academic Medical Centre, Amsterdam University, Amsterdam

Strumpf RK, Humphrey JD, Yin FC (1993) Biaxial mechanical properties of passive and tetanized canine diaphragm. J Biomech 265:469–475

Suso S, Vicente P, Angles F (1985) Surgical treatment of the non-functional spastic hand. J Hand Surg 10:54–56

Tardieu C, Huet de la Tour E, Bret MD, Tardieu G (1982) Muscle hypoextensibility in children with cerebral palsy: I. Clinical and experimental observations. Arch Phys Med Rehabilit 63:97–102

Trombitas K, Jin JP, Granzier H (1995) The mechanically active domain of titin in cardiac muscle. Circ Res 77:856–861

van der Linden BJJJ (1998) Mechanical modeling of muscle functioning. PhD Thesis in Faculty of Mechanical Engineering, University of Twente, Enschede, The Netherlands

Willems ME, Huijing PA (1994) Heterogeneity of mean sarcomere length in different fibres: effects on length range of active force production in rat muscle. Euro J Appl Physiol Occup Physiol 68:489–496

Wohlfart B, Grimm AF, Edman KA (1977) Relationship between sarcomere length and active force in rabbit papillary muscle. Acta Physiol Scand 101:155–164

Yucesoy CA, Koopman HJFM, Huijing PA, Grootenboer HJ (2002) Three-dimensional finite element modeling of skeletal muscle using a two-domain approach: linked fiber-matrix mesh model. Journal of Biomechanics 35:1253–1262

Yucesoy CA, Koopman HJFM, Baan GC, Grootenboer HJ, Huijing PA (2003) Extramuscular myofascial force transmission: experiments and finite element modeling. Arch Physiol Biochem 111:377–388

Yucesoy CA, Baan GC, Koopman HJFM, Grootenboer HJ, Huijing PA (2005) Pre-strained epimuscular connections cause muscular myofascial force transmission to affect properties of synergistic EHL and EDL muscles of the rat. J Biomech Eng 127:819–828

Yucesoy CA, Koopman HJFM, Grootenboer HJ, Huijing PA (2006a) Finite element modeling of aponeurotomy: altered intramuscular myofascial force transmission yields complex sarcomere length distributions determining acute effects. Biomech Model Mechanobiol (in press)

Yucesoy CA, Maas H, Koopman HJFM, Grootenboer HJ, Huijing PA (2006b) Finite element modeling of relative position of a muscle: effects of extramuscular myofascial force transmission. Med Eng Phys 28:214–226

Yucesoy CA, Maas H, Koopman HJFM, Grootenboer HJ, Huijing PA (2006c) Mechanisms causing effects of muscle position on proximo-distal muscle force differences in extra-muscular myofascial force transmission. Medical Engineering and Physics 28:214–226

Zuurbier CJ, Everard AJ, van der Wees P, Huijing PA (1994) Length-force characteristics of the aponeurosis in the passive and active muscle condition and in the isolated condition. J Biomech 27:445–453

Zuurbier CJ, Heslinga JW, Lee-de Groot MB, Van der Laarse WJ (1995) Mean sarcomere length-force relationship of rat muscle fibre bundles. J Biomech 28:83–87

Zwick EB, Saraph V, Zwick G, Steinwender C, Linhart W E, Steinwender G (2002) Medial hamstring lengthening in the presence of hip flexor tightness in spastic diplegia. Gait Posture 16:288–296